Construction and Building Materials 234 (2020) 117293

Contents lists available at ScienceDirect

Construction and Building Materials

journal homepage: www.elsevier.com/locate/conbuildmat

New empirical approach for determining nominal shear capacity of steel fiber reinforced concrete beams

Masoud Ahmadi [a], Ali Kheyroddin [b], Ahmad Dalvand [c], Mahdi Kioumarsi [d]

[a] Department of Civil Engineering, Ayatollah Boroujerdi University, Boroujerd, Iran
[b] Faculty of Civil Engineering, Semnan University, Semnan, Iran
[c] Department of Engineering, Lorestan University, Khorramabad, Iran
[d] Department of Civil Engineering and Energy Technology, OsloMet – Oslo Metropolitan University, Oslo, Norway

HIGHLIGHTS

- Nonlinear formulations for determining average shear stress of SFRC beams without stirrups are developed.
- All of the proposed models have acceptable ability to calculate average shear stress.
- The proposed approaches can be used as alternative methods to pre-shear design of SFRC beams.

ARTICLE INFO

Article history:
Received 3 February 2019
Received in revised form 2 October 2019
Accepted 14 October 2019

Keywords:
Steel fiber
Concrete
Shear
Beam
Empirical approach
ANNs
GEP

ABSTRACT

The main objective of this paper is to develop new design formulations for determining shear stress of steel fiber-reinforced concrete (SFRC) beams without stirrups using Gene Expression Programming (GEP) and Artificial Neural Networks (ANNs) based on a large number of test results. The proposed formulations relate the average shear stress to geometrical, and material properties of common reinforced concrete beam (effective depth, ratio of shear span to effective depth, compressive strength of concrete, and longitudinal steel reinforcement) and fiber properties (diameter, length, and volume percentage). In order to verify the validity and reliability of the proposed formulations, a comparative assessment was conducted between measured and calculated average shear stress of beams. The comparative assessment is carried out in terms of common and modified coefficient of determination (R and R_m), root- mean-square error (RMSE), mean absolute percentage error (MAPE), and gradients of regression lines (k and k'). The results obtained for the considered statistical measures and performance criteria reveal that all of the proposed formulations have acceptable ability to calculate average shear stress for a wide range of shear span to effective depth ratios.

1. Introduction

Fibers are mainly categorized into synthetic and natural substances. The sufficient quantity integration of discontinuous discrete fibers, with a randomly orientation into concrete mix, has remarkable advantage on performance of reinforced concrete (RC) members [1–5]. The choice of appropriate mixing procedure, type, and shape of the fibers have the main role to obtain the potential advantages such as ductility of concrete, and prevention of catastrophic diagonal tension failure [6]. Due to the well-substantiated advantages of steel fibers, steel fiber-reinforced concrete (SFRC) is progressively becoming applicable, especially in beams and slabs, to improve the performance of RC members [6–8]. The use of steel fibers with adequate strength to pullout, especially crimped and hooked fibers, has been extensively studied in recent years [9–13]. When tensile stress in RC beam exceeds the tensile capacity of concrete, micro-cracks are about to appear. A random orientation and distribution of steel fibers all over concrete transfers tensile stresses through the produced cracks and delay the growth of cracks size and their fast propagation in the beam [13–15]. Tensile stresses cause steel fiber to fracture or pullout the fiber from the cement matrix (breakdown of interfacial bond between fiber and concrete) [16]. As the consequence of improving in the post-cracking behavior, utilization of SFRC possesses superior behavior subjected to various types of loading condition—fibers impart increasing in characteristics such as ductility, shear capacity and toughness of beams—and changes the catastrophic brittle failure to ductile mode [17–20].

Similar to common reinforced concrete beams, the maximum shear stress of SFRC beams is attributable to effective depth (d),

https://doi.org/10.1016/j.conbuildmat.2019.117293
0950-0618/© 2019 The Author(s). Published by Elsevier Ltd.

the ratio of shear span to effective depth (a_v/d), and longitudinal steel reinforcement ratio (ρ). The larger effective depth of beam delays the formation of diagonal web-shear cracks, thereby leading to a greater shear capacity. The shear behavior of beams is appreciably affected by the a_v/d ratio. A higher value of a_v/d will result in a higher shear strength. It is worth mentioning that sufficient amount of longitudinal reinforcement guarantee the occurrence of the shear failure. Furthermore, the shear stress of SFRC beams depends on the volume percentage of fibers (V_{SF}), aspect ratio (ratio of length to diameter of fibers), and shape of the steel fibers [9,21–23].

2. Research significance

The shear behavior of SFRC beams is affected by various parameters such as steel fiber properties, bond, dimensions of beam, and concrete properties. Thereby, a precise calculation of shear stress of SFRC beams is an intricate problem that has not been fully understood yet. Thus, it is crucial for researchers to achieve a deep comprehension of shear behavior of SFRC beams. So far, researchers have developed models for determining ultimate shear stress of SFRC beams [21,24–28]. Some of these models have been driven from linear regression analysis and verified by a limited number of experimental results. Consequently, these are not able to calculate the average shear stress with sufficient precision and reliability for a wide range of a_v/d ratio.

Nowadays, researchers utilize various types of intelligence methods such as support vector machines, artificial neural networks (ANNs), Bayesian networks, genetic algorithms that used in a wide range of civil engineering applicants. One of the main problems in the usage of aforementioned methods is their convenience in engineering design methods [29–31]. Overcoming this challenge, researchers are seeking to utilize new approach that could generate design equations. The focus of this paper is to develop new design formulations for determining shear stress of SFRC beams without stirrups using Gene Expression Programming (GEP) and ANNs based on a large number of test results. The equation-based models may have a positive effect on the development of efficient design guidelines and the use of steel fibers in construction industry [32]. The proposed equations are function of the geometrical properties of RC beam, mechanical characteristics of concrete, and fiber properties.

3. Experimental database

So far, a large number of experimental studies have been carried out to identify the effect of various shape of steel fibers on shear behavior of steel fiber-reinforced concrete beams with no shear reinforcement and addressed key parameters that contribute to the purpose of this paper. The 129 experimental results are collected from the outcomes released in literatures that deal with the utilization of hooked and crimped steel fibers to improve the shear capacity of RC beams [12–14,21,24,27,33–39]. The experimental results meeting the following criteria were used in the present study:

- The beams should be tested under a monotonically increased concentrated load to avoid dynamic effects on failure.
- Beams failed in shear or with a crack pattern indicating that shear failure mode is predominant are collected.
- The compressive strength of concrete should be larger than 17 MPa.
- The longitudinal reinforcement ratios of selected beams are greater than 1% to secure shear failure rather than flexural failure.
- The amount of steel fiber is limited to 2%.

The key affecting parameters of database on average shear stress are effective depth (d), ratio of shear span to effective depth (a_v/d), ratio of longitudinal steel reinforcement (ρ), standard cylinder compression strength of concrete (f_c'), and steel fiber factor (F_{SF}). The F_{SF} is related to the diameter (D_{SF}), length (L_{SF}), and volume percentage (V_{SF}) of steel fibers, as expressed in Eq. (1) [9].

$$F_{SF} = V_{SF}L_{SF}/D_{SF} \tag{1}$$

It should also be emphasized that the amount of steel fiber is varied from 0.25 to 2. The statistical properties of the aforementioned variables including the measurement of central tendency and dispersion are calculated and presented in Table 1. The reference value of the key affecting parameters is selected to be close to the corresponding average value. Furthermore, Fig. 1 depicts the shear strength of SFRC beams as a function of key affecting parameters.

4. Development of ultimate shear stress formulations

In this section, four new design formulations for calculating the nominal average shear stress of SFRS beams without stirrups are developed using ANNs and GEP approaches. It should be noted that strength reduction factors for determining the shear stress is assumed one. Then, the assessment and comparison of results is conducted. It should be mentioned that, in the proposed equations, the size effect on shear strength of beams is not considered. The proposed models have acceptable efficiency in the aforementioned range of variations of the key affecting parameters, which are presented in Table 1.

4.1. ANN-Based Formulation

Artificial neural network is one of the efficient intelligent systems utilized as a reliable tool in various field of civil engineering [29,40,41]. To acquire the best network, the selection of appropriate set of input parameters is a big challenge. In the present study, five input parameters (d, a_v/d, ρ, f_c', and F_{SF}) are opted to build the ANN model. The preparation of training data and network training procedure are the main steps of constructing ANN. A multi-layer perceptron network is chosen for network creation. In order to model the efficient network, selection of a good transfer function, and adequate number of hidden layers and neurons are crucial [42,43]. In the first step, dataset is investigated with reference to the various percentage of training, verification, and test sets. In this step, the amount of training data is varied between 40- and 80-percent. The construction of network is repeated for several configurations to set the optimum condition. As a result, the parameters settings are presented as follow:

- Levenberg-Marquardt algorithm is utilized for network training function.
- A pure linear and tan-sigmoid function are implemented as the transfer function in the final and hidden layers, respectively.
- 60-percent of data is allocated to the training of the network, 20-percent to the validation step, and 20-percent to the testing phase.
- The regression values and mean squared error are opted as stop criteria.
- The eight neurons are used in the hidden layer.

Table 1
Statistical summary of database.

Descriptive Statistics	d (mm)	a_v/d	ρ (%)	f'_c (MPa)	F_{SF}	v (MPa)
Range	484	5	4.69	90.9	188.75	12.45
Mean	260.82	2.81	2.59	46.19	65.55	3.80
Variance	16450.8	0.71	1.35	355.18	1323.14	3.92
Std. Deviation	128.26	0.84	1.16	18.85	36.38	1.98
Coeff. Of Variation	0.49	0.3	0.45	0.41	0.56	0.52
Min	126	1.0	1.03	20.6	11.25	1.5
25th Percentile	167.5	2.0	1.92	31	40.63	2.61
50th Percentile	219	3	2.0	42.4	60	3.13
75th Percentile	340	3.43	2.9	49.2	82.5	4.54
Max	610	6	5.72	111.5	300	13.95
Reference Value	270	2.8	2.5	50	–	–

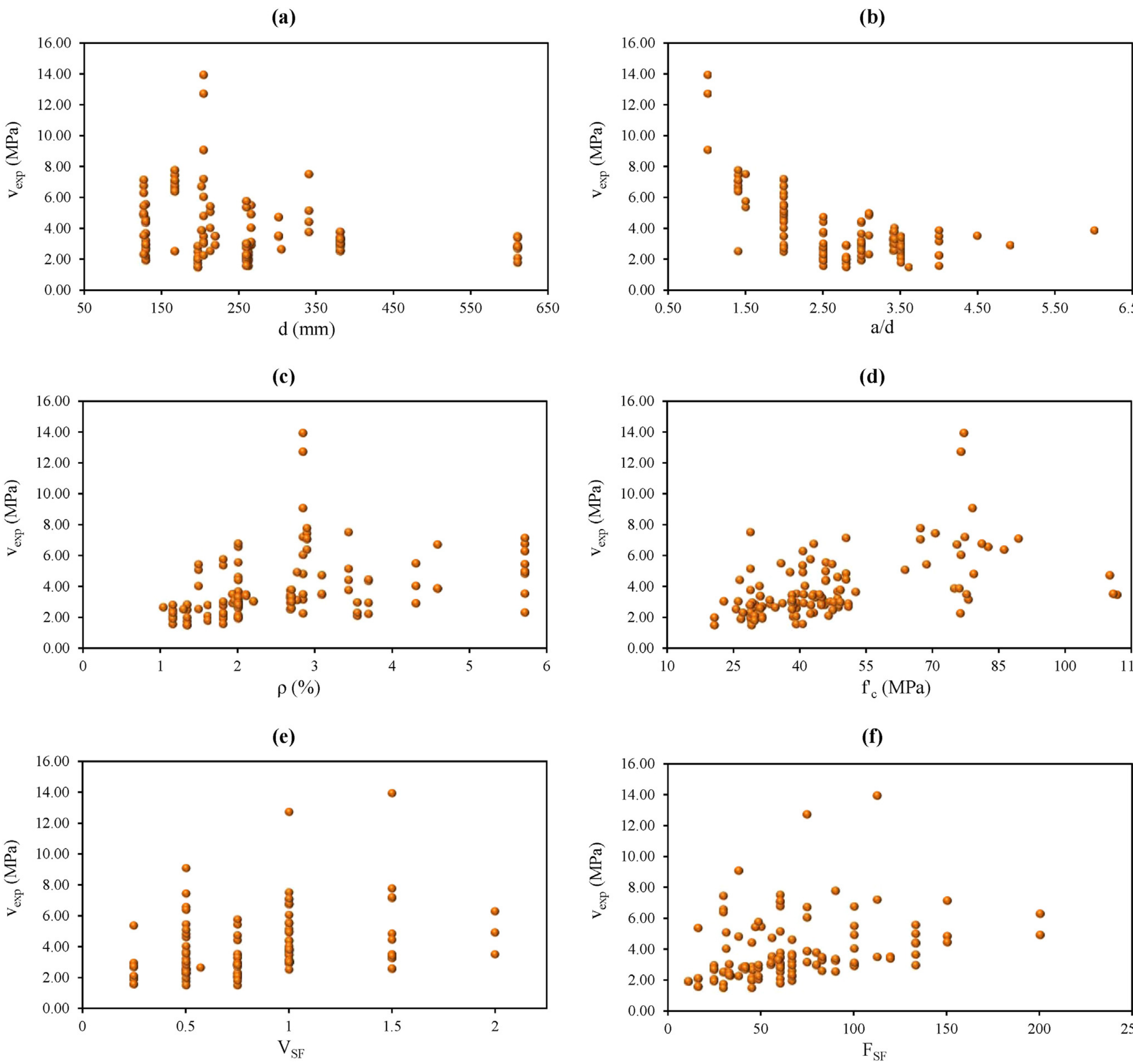

Fig. 1. Effect of key parameters on average shear stress.

The schematic configuration and performance of the optimum network are shown in Figs. 2–3.

The amount of regression values with corresponding to the optimum network are 0.979, 0.988, and 0.968 for training, verification and test sets. The basic structure of the proposed ANN-based formulation is expressed in the following:

$$v_1 = C_d C_{a_v/d} C_\rho C_{f'_c} v_{SFRC} \quad (2)$$

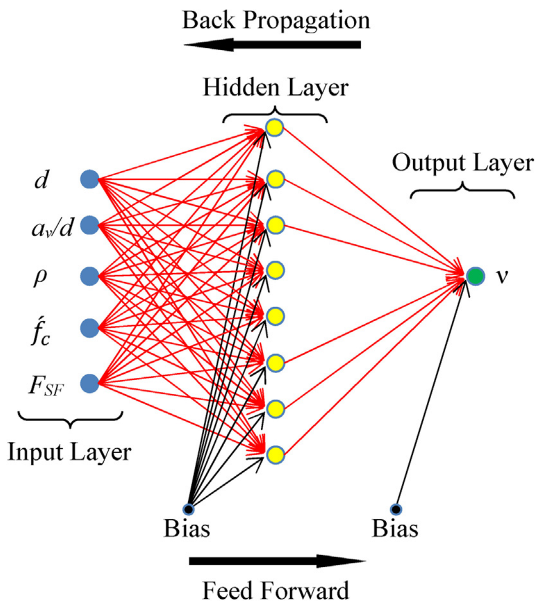

Fig. 2. Schematic configuration optimum network.

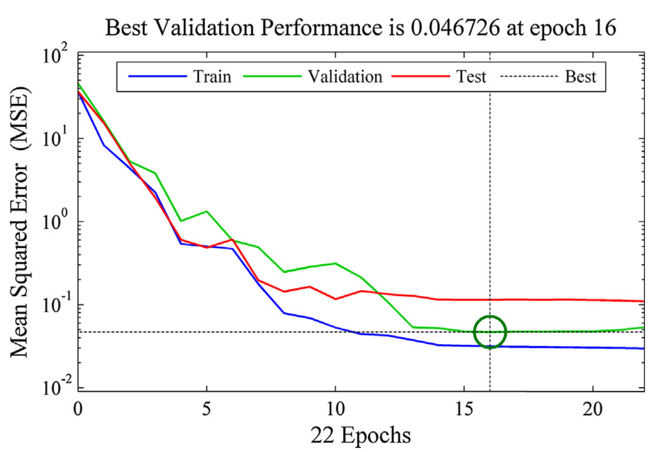

Fig. 3. Performance of optimum network.

$$C_d = C\left(a_v/d,\ \rho,\ f_c'\right) \quad (3)$$

$$C_{a_v/d} = C\left(d,\ \ \rho,\ \ f_c'\right)$$

$$C_{\ \rho} = C\left(d,\ a_v/d,\ f_c'\right)$$

$$C_{f_c'} = C(d, a_v/d, \rho)$$

The considered procedure to characterize the affected parameters in Eq. (2) was introduced by Leung et al. [30]. In this equation, C_d, $C_{a_v/d}$, C_ρ, and $C_{f_c'}$ are considered as correction factors. In order to calculate v_{SFRC}, it is assumed that the variation of F_{SF} is independent and other input parameters are set to the corresponding reference values as in Fig. 4.

To determine the correction factor C_d, three sets of curves should be generated with different values of d from minimum to maximum. In the first set, master curves are specified with various discrete values of a_v/d ratio, whereas the values of other parameters (ρ and f_c') are fixed at the corresponding reference values, see Fig. 5a. The number of curves is equal to 12 data series. Deriving the output value of network by the value of read off from the master curves, the correction factor C_d can be calculated.

Similar to the mentioned procedure, the effects of ρ and f_c' on the variation of C_d are presented in Fig. 5b and c. Based on the three sets of the obtained curves for C_d, see Fig. 5a–c, one main curve using the minimum least square error that fits the mean values of it was found. The same procedure has been utilized to determine the other correction factors ($C_{a_v/d}$. , $C_{\ \rho}$, and $C_{f_c'}$). The master curvefor $C_{\ \rho}$ are shown in Fig. 6. Owing to space limitation, the results for other correction factors ($C_{a_v/d}$ and $C_{f_c'}$) will not be discussed in detail here.

As the consequence of the above mentioned approach, the following formulations have been established:

$$C(d) = -0.23\left(\frac{d}{270}\right)^4 + 0.8\left(\frac{d}{270}\right)^3 - 1.04\left(\frac{d}{270}\right)^2 + 0.94\frac{d}{270} + 0.53 \quad (4)$$

$$C(a_v/d) = 1.14\left(\frac{a_v}{2.8d}\right)^4 - 6.94\left(\frac{a_v}{2.8d}\right)^3 + 15.67\left(\frac{a_v}{2.8d}\right)^2 - 15.8\frac{a_v}{2.8d} + 6.89 \quad (5)$$

$$C(\rho) = 0.225\frac{\rho}{2.5} + 0.778 \quad (6)$$

$$C(f_c') = -0.83\left(\frac{f_c'}{50}\right)^6 + 7.17\left(\frac{f_c'}{50}\right)^5 - 23.756\left(\frac{f_c'}{50}\right)^4 + 37.96\left(\frac{f_c'}{50}\right)^3 - 30.45\left(\frac{f_c'}{50}\right)^2 + 12.03\frac{f_c'}{50} - 1.126 \quad (7)$$

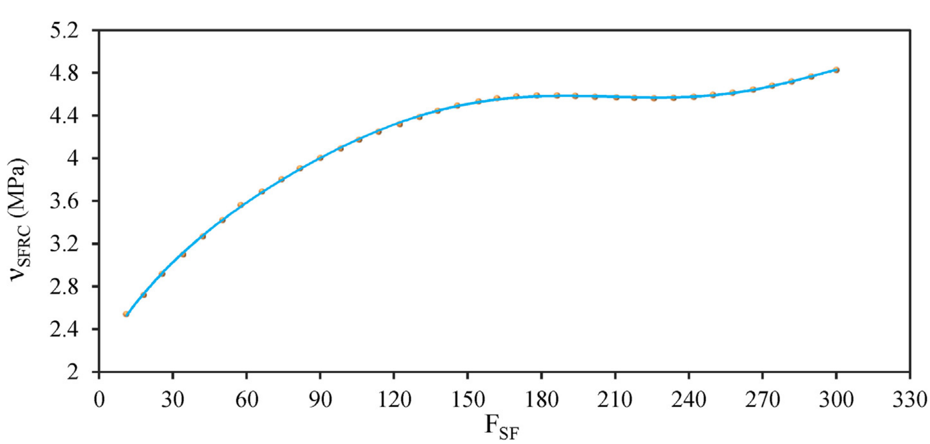

Fig. 4. Variation of v_{SFRC} with respect to steel fiber factor.

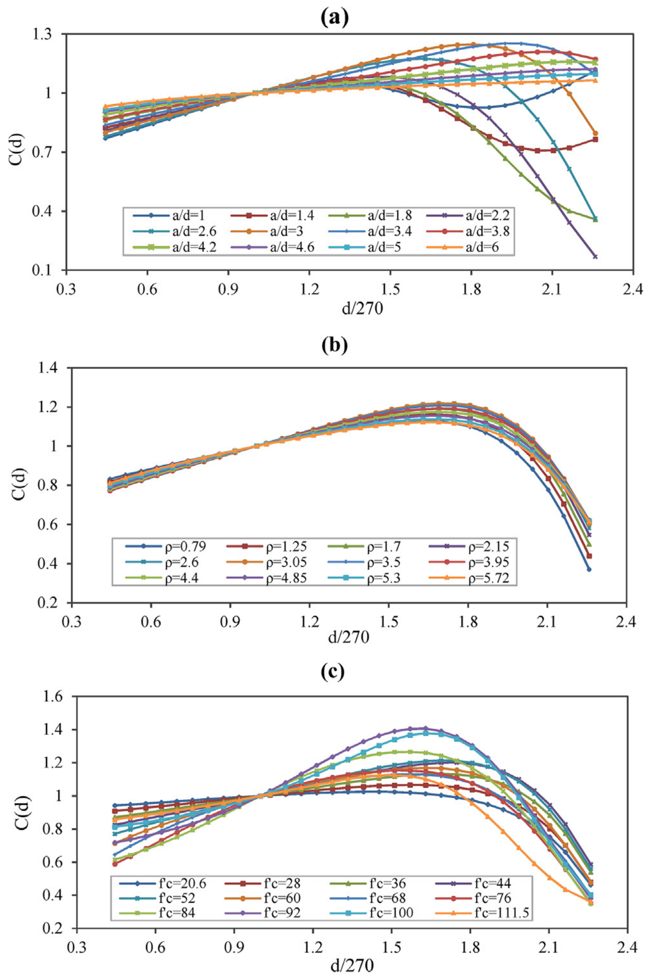

Fig. 5. Variation of C_d with respect to a_v/d, ρ, and f'_c.

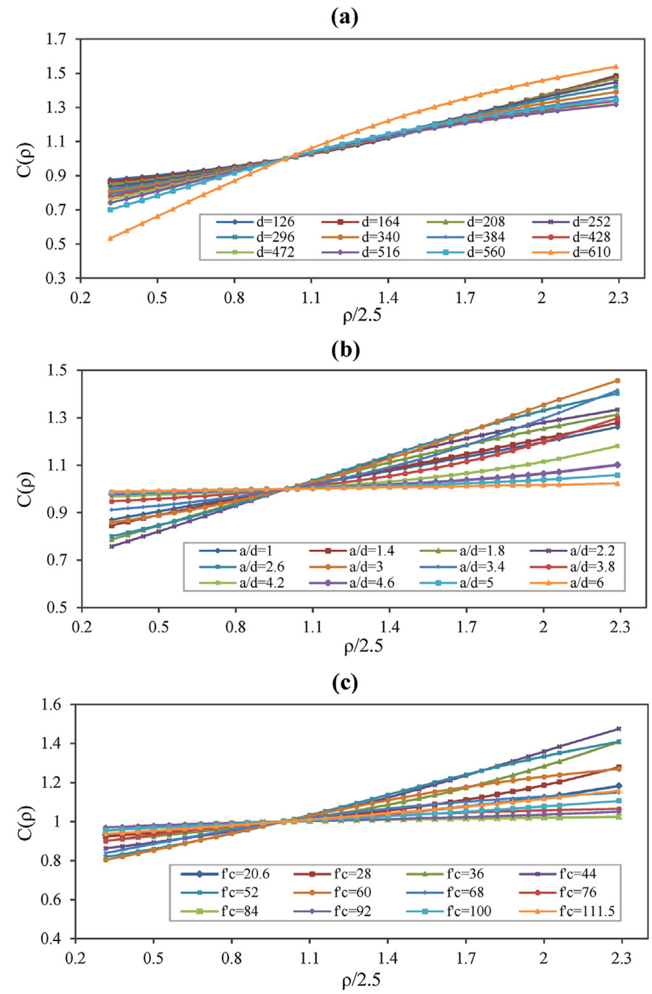

Fig. 6. Variation of C_ρ with respect to $d, a_v/d$, and f'_c.

4.2. GEP-Based Formulation

GEP approach was proposed by Ferreira et al. [44] in 2001, based on genetic algorithm (GA). GEP is more efficient than GA and genetic programing (GP) for function funding problems. GP—a subset of machine learning—was developed by Cramer in 1985, and was developed by Koza in 1992. In GEP, the linear chromosomes are considered as genotype and the parse trees as phenotype. Furthermore, GEP is a complex tree structure in which the chromosomes are expressed as an expression tree (ET). Karva language was developed specifically at the sake of reading and expressing the information encoded in the chromosomes.

In this paper, three new formulations are developed by the GEP approach to specify average shear stress of SFRC beam without stirrups at the final stage of loading:

$$v_{GEP} = v\left(C_d,\ C_{a_v/d},\ C_\rho,\ C_{f'_c}\right) \tag{8}$$

In order to interdict the effect of overfitting, a maximum 70-percent of the whole datasets is utilized for the learning phase and the others used to the test stage. The root mean square error (RMSE) is a common index that measures the differences between predicted and main amount of target. RMSE is selected as a fitness function. The three independent formulations for shear stress can be expressed as Eqs. (9)–(11).

$$v_2 = d/a_v\left(\frac{F_{SF}}{d} + 0.555\sqrt{\rho f'_c} + 1\right) + 1 \tag{9}$$

$$v_3 = \rho - \frac{37.957\frac{a_v}{d}\rho}{d + F_{SF} - 10.57} + \frac{d + f_c'^2}{9.44\frac{a_v}{d}f'_c} \tag{10}$$

$$v_4 = 0.095\frac{f'_c}{\frac{a_v}{d}} + \frac{\rho - 0.137}{\frac{a_v}{d} - 0.395} + \frac{0.108d + F_{SF}}{f'_c - \frac{a_v}{d} + 85.256} \tag{11}$$

Due to space limitations, on adjusted input parameters and corresponding expression tree for v_2 and v_4 are shown in Tables 2 and Figs. 7–8.

5. Reliability assessment of the developed models

5.1. Verification of proposed formulations

To examine the reliability and precision of the four proposed new design formulation, their outcomes were compared to the collected experimental database. The comparison of the results of formulations with the experimental results and the residual values of the four proposed formulations are depicted in Figs. 9–10.

Although the ANN-based formulation has more complexity, it is shown that this model has the lowest dispersal in comparison with other models. The highest dispersal belongs to the second formulation where it predicts shear capacity with a more uncertainty than other formulations. Due to different categories of training dataset in GEP formulations, the results of them is not exactly the same. Furthermore, the first and fourth formulations underestimated

Table 2
Parameters settings for v_2 and v_4.

Parameter	v_2	v_4
General		
Training Records	73	85
Validation Records	56	44
Chromosomes	30	37
Genes	3	3
Head size	6	8
Tail size	7	9
Dc size	7	9
Gene size	20	26
Linking function	Addition	Addition
Function	+, −, /, *, Sqrt, and Inv	+, −, /, *, and Inv
Genetic operators		
Function Insertion	0.00206	0.00635
Permutation	0.00546	0.0082
Inversion	0.00546	0.0082
Gene Recombination	0.00277	0.0028
Gene Transposition	0.00277	0.0028
Dc Mutation	0.00206	0.00268
Dc Permutation	0.00546	0.0082
Dc Inversion	0.00546	0.0082
Numerical constant		
Constants per Gene	10	10
Data Type	Floating-Point	Floating-Point
Lower Bound	−10	−10
Upper Bound	10	10

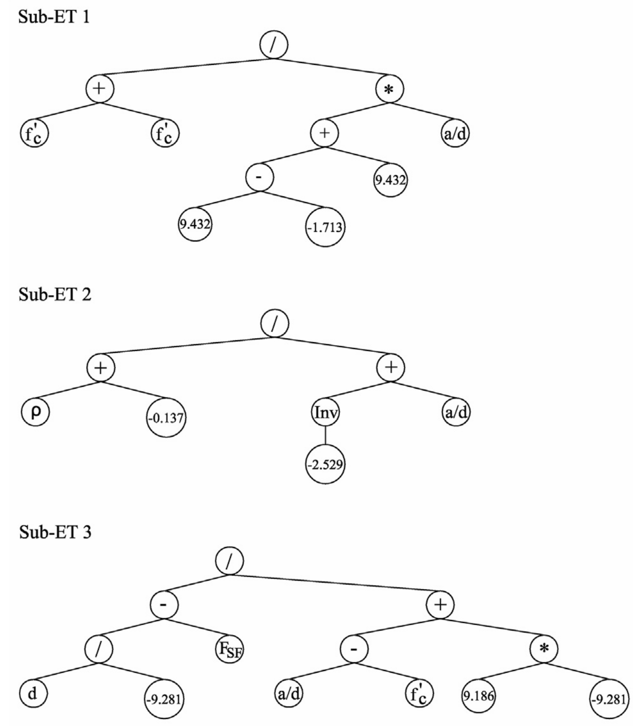

Fig. 8. ET corresponding to fourth formulation (v_4).

the shear capacity of beams for a spread range of data. Generally, the four presented formulations are able to calculate average shear stress of SFRC beams without stirrups appropriately.

To assess reliability of the developed formulations more accurately, i) three well-known statistical measures; coefficient of determination (R^2) —that represents a meter of how well experimented data are estimated by the proposed approach—root mean square error (RMSE) and mean absolute percentage error (MAPE), that quantified accuracy and goodness of fit, and ii) the factors presented by [45] and [46] were utilized. These statistical indices can be calculated using equations summarized in Tables 3 [47].

where $v_{i,actual}$ is the actual value of average shear stress, $\bar{v}_{actual}$ is the mean of all values of $v_{i,actual}$, $v_{i,model}$ is the value of the average shear stress obtained from the proposed model, $\bar{v}_{model}$ is the mean of all amounts of $v_{i,model}$, n is the number of specimens, k and k' are the gradients of regression lines across the center, R_o^2 and $R_o'^2$ are correlation coefficients of regression lines related to actual and predicted values, and r_m^2 is the modified index of R^2.

Results of the three statistical measures are presented in Table 4. Considering the ideal condition, the corresponding values of MAPE, RMSE and R, are equal to, zero, zero and one, respectively. The findings by Smith [48] have substantiated that satisfactory condition can be achieved if the square root of coefficient of determination is greater than 0.8 and the differences between experimented and predicted values are the lowest. Results demonstrate that the first and fourth models have accurate predictions ability. MPAE values corresponding to them are 12.73 and 11.27, respectively. In addition, the second equation has less efficiency because of low R-value and maximum value of MAPE.

Furthermore, Table 5 shows the results of the performance criteria. There are reasonable convergence between the actual and estimated values by four new design formulations. It can be found that all the formulations pass desired conditions and could estimate the average shear stress of the SFRC beams with a good degree of accuracy. The results of comparison reveal that the first and forth equations have best efficiency among all of the proposed modes and provide the best performance.

5.2. Comparison with existing equations

To assess the accuracy of the proposed shear formulations, the predicted values are compared with the five popular existing equations against the 74 experimental specimens presented in the database. It should be noted that strength reduction factors in all equations are equal to one. The shear equations developed by ACI 544.4R [49], Narayanan and Darwish [24], Khuntia et al. [28],

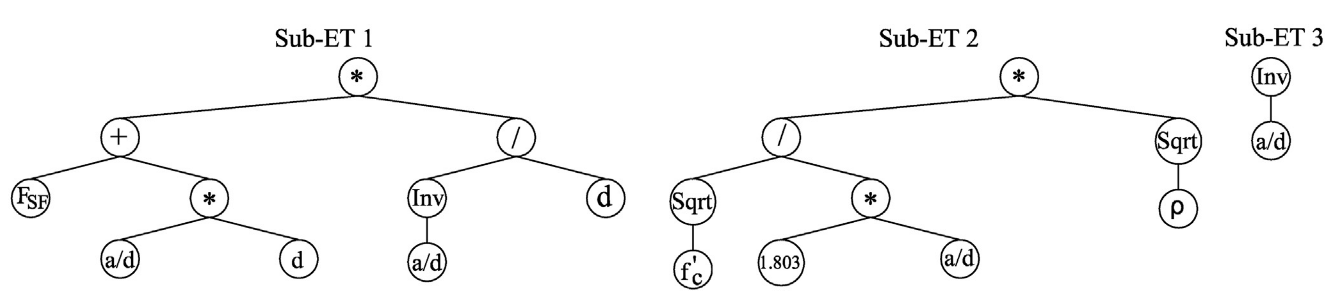

Fig. 7. ET corresponding to second formulation (v_2).

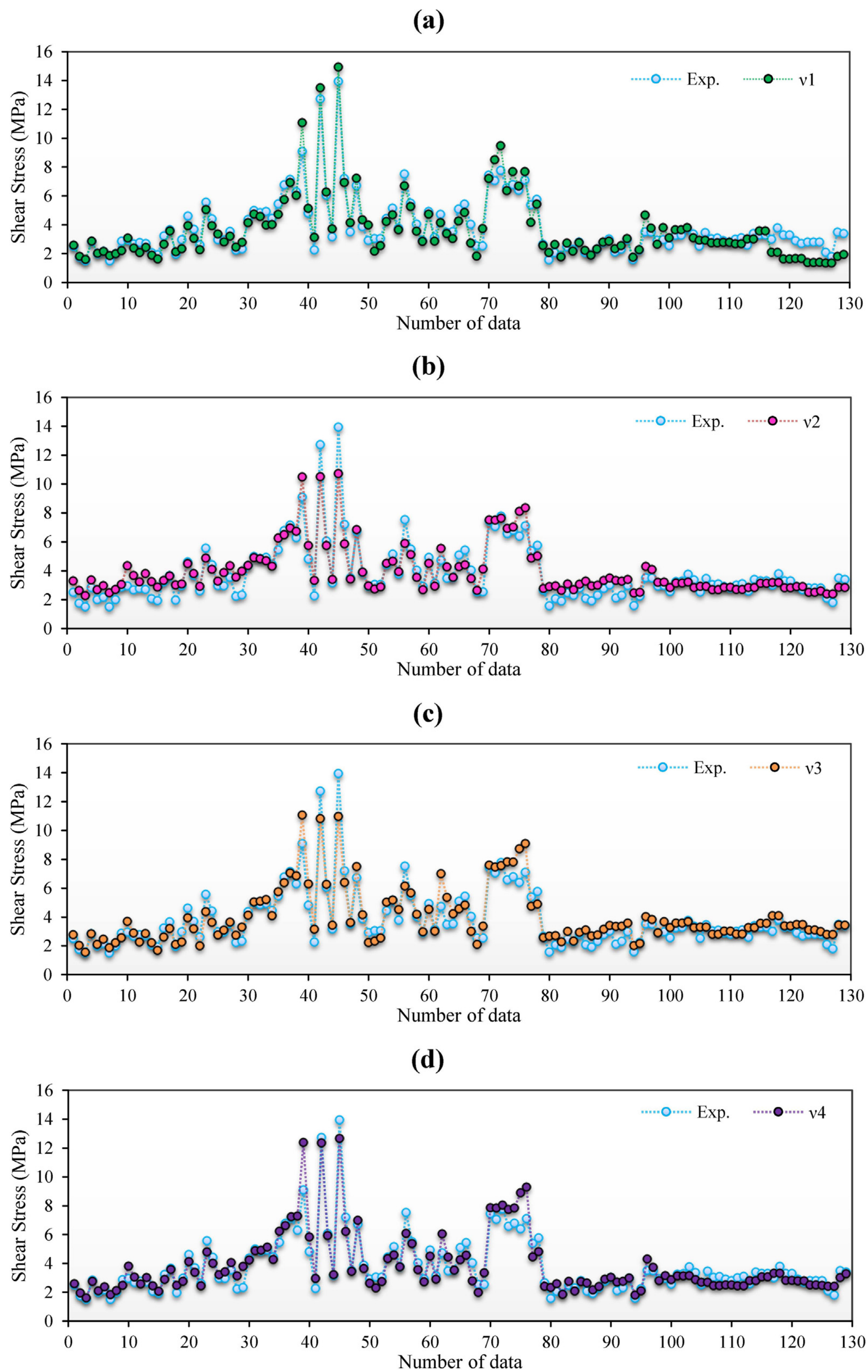

Fig. 9. Comparison of predicted versus experimental results: a) first formulation (v_1), b) second formulation (v_2), c) third formulation (v_3), and d) fourth formulation (v_4).

Yakoub [14] and Kwak et al. [21] are utilized for comparison. Four statistical measures were utilized to compare the results of developed formulations: standard deviation, mean, and coefficient of variation (COV) of the performance ratio ($\frac{v_{exp.}}{v_{pred.}}$)—taken as understandable measures—and MPAE of predicted results. The selection of MAPE value is related to its result interpretability and scale-independency. The ideal condition is achieved when small standard deviation is accompanied by a value of mean close to one.

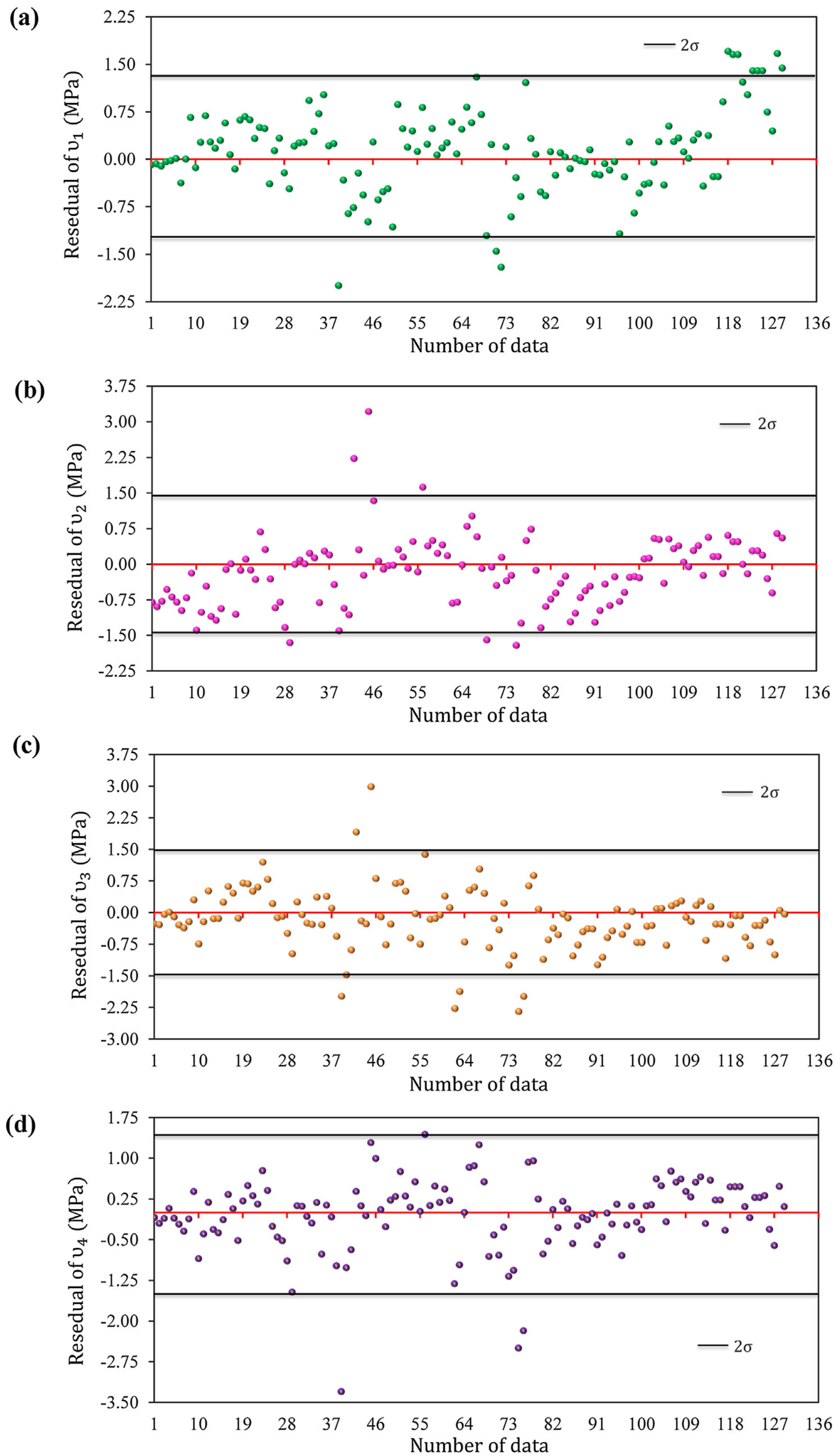

Fig. 10. Residual values of the four developed formulations: a) first formulation (v_1), b) second formulation (v_2), c) third formulation (v_3), and d) fourth formulation (v_4).

The smallest value of MAPE indicates the suitable accuracy to provide the appropriate prediction performance. Table 6 compares the statistical measures of test results on developed formulations and exiting equations. The standard deviation, COV, and MAPE of fourth formulation are 0.152, 14.674, and 12.641, respectively, which are lower than those of other equations. By analyzing the results in

Table 3
Equations of Statistical indices.

Statistical index	Expression model	
R^2	$\frac{\left[\sum_{i=1}^{n}\left(v_{i,actual}-\bar{v}_{actual}\right)\left(v_{i,model}-\bar{v}_{model}\right)\right]^2}{\sum_{i=1}^{n}\left(v_{i,actual}-\bar{v}_{actual}\right)^2\sum_{i=1}^{n}\left(v_{i,model}-\bar{v}_{model}\right)^2}$	(12)
$RMSE$	$\sqrt{\frac{\sum_{i=1}^{n}\left(v_{i,actual}-v_{i,model}\right)^2}{n}}$	(13)
$MAPE$	$\left(\frac{100}{n}\right)\sum_{i=1}^{n}\left(\frac{\lvert v_{i,actual}-v_{i,model}\rvert}{v_{i,actual}}\right)$	(14)
k	$\frac{\sum_{i=1}^{n}v_{i,actual}v_{i,model}}{\sum_{i=1}^{n}v_{i,model}^2}$	(15)
k'	$\frac{\sum_{i=1}^{n}v_{i,actual}v_{i,model}}{\sum_{i=1}^{n}v_{i,actual}^2}$	(16)
R_o^2	$1-\frac{\sum_{i=1}^{n}\left(v_{i,model}-v_i^{ro}\right)^2}{\sum_{i=1}^{n}\left(v_{i,model}-\bar{v}_{model}\right)^2}$	(17)
$R_o'^2$	$1-\frac{\sum_{i=1}^{n}\left(v_{i,actual}-\hat{v}_i^{ro}\right)^2}{\sum_{i=1}^{n}\left(v_{i,actual}-\bar{v}_{actual}\right)^2}$	(18)
v_i^{ro}	$kv_{i,model}$	(19)
$\hat{v}_i^{ro}$	$k'v_{i,actual}$	(20)
r_m^2	$R^2\left(1-\sqrt{\lvert R^2-R_o^2\rvert}\right)$	(21)

Table 4
Statistical indices (MAPE, RMSE and R) for proposed models.

Indicator	First model	Second model	Third model	Forth model
R	0.954	0.932	0.93	0.947
RMSE (kN)	0.636	0.703	0.70	0.627
MPAE	12.73	16.03	13.49	11.27

Table 5
Performance criteria of developed models.

Criteria	Condition	First formulation	Second formulation	Third formulation	Forth formulation
R	R > 0.8	0.954	0.932	0.93	0.947
k	0.85 < k < 1.15	0.991	0.975	0.957	0.967
k'	0.85 < k' < 1.15	0.983	0.993	1.013	1.0
R_m	R_m > 0.5	0.8	0.748	0.75	0.785
Overall Performance		O.K	O.K	O.K	O.K

Table 6
Statistical measures of the predicted values against experimental specimens.

Author	Number of data	Formulation	$\frac{v_{exp.}}{v_{pred.}}$			MAPE (%)
			Mean	Std. Deviation	COV (%)	
Ashour et al. [27]		Formulation 01	0.88	0.09	10.59	14.92
		Formulation 02	1.01	0.18	17.44	13.17
		Formulation 03	0.99	0.19	19.33	16.28
		Formulation 04	0.98	0.14	13.98	11.59
	12	ACI 544.4R	1.13	0.36	32.06	19.12
		Narayanan and Darwish	0.99	0.15	15.21	13.55
		Khuntia et al.	1.46	0.37	25.22	27.77
		Kwak et al.	0.87	0.11	12.62	17.59
		Yakoub	1.21	0.28	23.02	23.29
Swamy et al. [34]		Formulation 01	1.06	0.05	4.40	5.62
		Formulation 02	1.08	0.03	2.80	7.77
		Formulation 03	1.00	0.05	5.19	4.14
		Formulation 04	1.08	0.04	3.85	6.91
	5	ACI 544.4R	1.33	0.21	16.16	23.30
		Narayanan and Darwish	1.06	0.09	8.72	8.35
		Khuntia et al.	1.55	0.25	15.95	34.05
		Kwak et al.	1.10	0.09	8.12	9.35
		Yakoub	1.55	0.25	15.95	34.05

(continued on next page)

Table 6 (*continued*)

Author	Number of data	Formulation	$\frac{v_{exp.}}{v_{pred.}}$ Mean	Std. Deviation	COV (%)	MAPE (%)
Kwak et al. [21]	4	Formulation 01	1.29	0.16	12.76	21.69
		Formulation 02	1.14	0.12	10.31	13.08
		Formulation 03	1.20	0.11	8.86	16.17
		Formulation 04	1.28	0.12	9.42	21.37
		ACI 544.4R	1.09	0.11	10.33	7.15
		Narayanan and Darwish	1.69	0.08	4.59	40.82
		Khuntia et al.	1.34	0.11	8.20	25.02
		Kwak et al.	1.38	0.08	6.01	27.07
		Yakoub	1.82	0.19	10.55	44.47
Dupont and Vandewalle [36]	19	Formulation 01	0.98	0.12	11.81	8.69
		Formulation 02	0.80	0.16	20.12	31.71
		Formulation 03	0.86	0.17	19.39	24.70
		Formulation 04	0.96	0.15	15.26	13.65
		ACI 544.4R	1.27	0.31	24.58	22.09
		Narayanan and Darwish	1.25	0.17	13.31	18.58
		Khuntia et al.	1.34	0.41	30.23	27.17
		Kwak et al.	1.06	0.12	11.26	10.19
		Yakoub	1.38	0.25	18.39	25.88
Cucchiara et al. [37]	3	Formulation 01	0.93	0.17	18.77	16.66
		Formulation 02	0.86	0.05	5.37	16.13
		Formulation 03	0.93	0.07	7.25	8.10
		Formulation 04	0.93	0.11	11.92	10.89
		ACI 544.4R	1.09	0.11	10.20	7.93
		Narayanan and Darwish	1.05	0.21	20.27	16.52
		Khuntia et al.	1.56	0.05	3.21	35.85
		Kwak et al.	0.93	0.17	17.81	15.79
		Yakoub	1.25	0.21	16.80	18.31
Montesinos [14]	10	Formulation 01	0.97	0.14	14.50	13.43
		Formulation 02	1.06	0.12	11.67	11.15
		Formulation 03	0.95	0.13	13.41	12.73
		Formulation 04	1.10	0.14	13.15	12.48
		ACI 544.4R	1.12	0.19	17.37	14.99
		Narayanan and Darwish	1.18	0.18	15.45	15.52
		Khuntia et al.	1.18	0.32	27.20	25.39
		Kwak et al.	1.21	0.17	14.26	16.71
		Yakoub	1.41	0.18	13.00	28.11
Dinh et al. [13]	21	Formulation 01	1.49	0.43	28.63	29.90
		Formulation 02	1.06	0.13	11.89	10.96
		Formulation 03	0.91	0.12	12.77	13.79
		Formulation 04	1.08	0.13	12.08	12.36
		ACI 544.4R	1.28	0.30	23.22	22.90
		Narayanan and Darwish	0.87	0.04	4.67	15.56
		Khuntia et al.	1.23	0.29	23.90	19.07
		Kwak et al.	0.86	0.07	8.57	16.76
		Yakoub	0.98	0.09	9.60	7.38
Global performance		Formulation 01	1.12	0.34	30.56	17.18
		Formulation 02	0.98	0.18	18.07	16.78
		Formulation 03	0.94	0.16	16.96	16.09
		Formulation 04	1.04	0.15	14.67	12.64
		ACI 544.4R	1.22	0.29	23.67	19.58
		Narayanan and Darwish	1.10	0.25	22.51	16.92
		Khuntia et al.	1.33	0.34	25.55	25.43
		Kwak et al.	1.01	0.19	18.79	15.23
		Yakoub	1.28	0.31	23.90	21.76

detail, it can be revealed that in more than 94 percent of data the MAPE of fourth model is<15%. The equations proposed by Khuntia et al. [28] and Yakoub [14] are more conservative than other equations studied in the paper. The mean value of the performance ratio for these equations are 1.33 and 1.28, respectively. In total, it can be noted that the proposed shear formulations produced more precise results in comparison with other existing equations.

6. Conclusion

In this paper, four new nonlinear empirical formulas are developed to determine the average shear stress of SFRC beams without stirrups based on a massive experimental database with considering a wide range of key affecting variables using two efficient computational intelligence approaches called gene expression programing and artificial neural networks. Five effective variables include steel fiber factor, effective depth, ratio of shear span to effective depth, standard cylinder compression strength of concrete, and longitudinal steel reinforcement. The detailed comparative assessment of the performance of proposed formulations is carried out in terms of common and modified coefficient of determination (R and R_m), root- mean-square error (RMSE), mean absolute percentage error (MAPE), and gradients of regression lines (k and k'). Results of this study have been verified based on the aforementioned range of key affecting parameters and the proposed models have acceptable efficiency in these ranges.

The following conclusions can be made based on the investigation:

- It can be concluded from the results that the first and fourth models provide more precision than other models. The R and MAPE values of the first formula are equal to 0.954 and12.73, respectively for all of the collected data. Furthermore, the corresponding values for fourth formula are equal to 0.947 and11.27, respectively.
- The comparison of the proposed formulations with existing well-Known equations which are ACI 544.4R, Narayanan and Darwish, Khuntia et al., Yakoub and Kwak et al. using 74 data from experimental database reveal that fourth model produced more precise results than other models. The standard deviation, COV, and MAPE of the fourth formulation are lower than those of the other formulations.
- The findings demonstrate that all of the empirical approaches provide reliable formulations with a useful application as alternative method to pre-shear design of SFRC beam.

While this study attempts to propose new design formulations based on a wide range of test results, further investigations are needed for their practical implementation such as the influence of size effect on shear strength in future works.

Declaration of Competing Interest

The authors declare that they have no known competing financial interests or personal relationships that could have appeared to influence the work reported in this paper.

Appendix A. Supplementary data

Supplementary data to this article can be found online at https://doi.org/10.1016/j.conbuildmat.2019.117293.

References

[1] H. Ju, K.S. Kim, D.H. Lee, J.-H. Hwang, S.-H. Choi, Y.-H. Oh, Torsional responses of steel fiber-reinforced concrete members, Compos. Struct. 129 (2015) 143–156.

[2] S. Abbas, A.M. Soliman, M.L. Nehdi, Exploring mechanical and durability properties of ultra-high performance concrete incorporating various steel fiber lengths and dosages, Constr. Build. Mater. 75 (2015) 429–441.

[3] D.-Y. Yoo, J.-M. Yang, Effects of stirrup, steel fiber, and beam size on shear behavior of high-strength concrete beams, Cem. Concr. Compos. (2017).

[4] M. Halimi, H. Sarkardeh, H. Bakhshi, M. Kioumarsi, Numerical investigation on effects of steel fibers content on flexural behavior of UHPCC, in: Adv. Eng. Mater. Struct. Syst. Innov. Mech. Appl. Proc. 7th Int. Conf. Struct. Eng. Mech. Comput. (SEMC 2019), CRC Press, Cape Town, South Africa, 2019, p. 1403.

[5] H. Kazemi, M. Zarghani, H. Sarkardeh, M. Kioumarsi, Numerical simulation of reinforced concrete cut-off wall with steel fibers under dam, in: SynerCrete'18 Interdiscip. Approaches Cem. Mater. Struct. Concr. Synerg. Expert. Bridg. Scales Sp. Time, Portugal, 2018: pp. 975–980.

[6] ACI Committee 544. State of the Art Report on Fiber Reinforced Concrete Reported (Reapproved 2002), 2002.

[7] H. Salehian, J.A.O. Barros, Prediction of the load carrying capacity of elevated steel fibre reinforced concrete slabs, Compos. Struct. 170 (2017) 169–191.

[8] A. Venkateshwaran, K.H. Tan, Arching Action in Steel Fiber-Reinforced Concrete Flat Slabs, ACI Struct. J. 115 (2018).

[9] H. Aoude, M. Belghiti, W.D. Cook, D. Mitchell, Response of steel fiber-reinforced concrete beams with and without stirrups, ACI Struct. J. 109 (2012) 359.

[10] M.G. Alberti, A. Enfedaque, J.C. Gálvez, Fibre reinforced concrete with a combination of polyolefin and steel-hooked fibres, Compos. Struct. 171 (2017) 317–325.

[11] B.W. Xu, J.W. Ju, H.S. Shi, Progressive micromechanical modeling for pullout energy of hooked-end steel fiber in cement-based composites, Int. J. Damage Mech. 20 (2011) 922–938.

[12] S.-H. Cho, Y.-I. Kim, Effects of steel fibers on short beams loaded in shear, Struct. J. 100 (2003) 765–774.

[13] H.H. Dinh, G.J. Parra-Montesinos, J.K. Wight, Shear Behavior of Steel Fiber-Reinforced Concrete Beams without Stirrup Reinforcement, ACI Struct. J. 107 (2010).

[14] H.E. Yakoub, Shear stress prediction: steel fiber-reinforced concrete beams without stirrups, ACI Struct. J. 108 (2011) 304.

[15] J.M. Torrents, A. Blanco, P. Pujadas, A. Aguado, P. Juan-García, M.Á. Sánchez-Moragues, Inductive method for assessing the amount and orientation of steel fibers in concrete, Mater. Struct. 45 (2012) 1577–1592.

[16] T. Soetens, A. Van Gysel, S. Matthys, L. Taerwe, A semi-analytical model to predict the pull-out behaviour of inclined hooked-end steel fibres, Constr. Build. Mater. 43 (2013) 253–265.

[17] O. Düğenci, T. Haktanir, F. Altun, Experimental research for the effect of high temperature on the mechanical properties of steel fiber-reinforced concrete, Constr. Build. Mater. 75 (2015) 82–88.

[18] B. Isojeh, M. El-Zeghayar, F.J. Vecchio, Fatigue behavior of steel fiber concrete in direct tension, J. Mater. Civ. Eng. 29 (2017) 4017130.

[19] W. Zhang, S. Chen, Y. Liu, Effect of weight and drop height of hammer on the flexural impact performance of fiber-reinforced concrete, Constr. Build. Mater. 140 (2017) 31–35.

[20] A. Kheyroddin, M. Ahmadi, M. Kioumarsi, Using Intelligent System Approach for Shear Strength Forecasting of Steel Fiber-Reinforced Concrete Beams, in: SynerCrete'18 Interdiscip. Approaches Cem. Mater. Struct. Concr. Synerg. Expert. Bridg. Scales Sp. Time., 2018.

[21] Y.-K. Kwak, M.O. Eberhard, W.-S. Kim, J. Kim, Shear strength of steel fiber-reinforced concrete beams without stirrups, ACI Struct. J. 99 (2002) 530–538.

[22] F. Zhang, Y. Ding, J. Xu, Y. Zhang, W. Zhu, Y. Shi, Shear strength prediction for steel fiber reinforced concrete beams without stirrups, Eng. Struct. 127 (2016) 101–116.

[23] E.O.L. Lantsoght, Database of shear experiments on steel fiber reinforced concrete beams without stirrups, Materials (Basel) 12 (2019) 917.

[24] R. Narayanan, I.Y.S. Darwish, Use of steel fibers as shear reinforcement, Struct. J. 84 (1987) 216–227.

[25] A.K. Sharma Shear, strength of steel fiber reinforced concrete beams, J. Proc. (1986) 624–628.

[26] M. Imam, L. Vandewalle, F. Mortelmans, D. Van Gemert, Shear domain of fibre-reinforced high-strength concrete beams, Eng. Struct. 19 (1997) 738–747.

[27] S.A. Ashour, G.S. Hasanain, F.F. Wafa, Shear behavior of high-strength fiber reinforced concrete beams, Struct. J. 89 (1992) 176–184.

[28] M. Khuntia, B. Stojadinovic, S.C. Goel, Shear strength of normal and high-strength fiber reinforced concrete beams without stirrups, Struct. J. 96 (1999) 282–289.

[29] M. Ahmadi, H. Naderpour, A. Kheyroddin, Utilization of artificial neural networks to prediction of the capacity of CCFT short columns subject to short term axial load, Arch. Civ. Mech. Eng. 14 (2014) 510–517.

[30] C.K. Leung, M.Y. Ng, H.C. Luk, Empirical approach for determining ultimate FRP strain in FRP-strengthened concrete beams, J. Compos. Constr. 10 (2006) 125–138.

[31] A. Kheyroddin, H. Naderpour, M. Ahmadi, Compressive strength of confined concrete in CCFST columns, J. Rehabil. Civ. Eng. 2 (2014) 106–113.

[32] E. Slater, M. Moni, M.S. Alam, Predicting the shear strength of steel fiber reinforced concrete beams, Constr. Build. Mater. 26 (2012) 423–436.

[33] K.H. Tan, K. Murugappan, P. Paramasivam, Shear behavior of steel fiber reinforced concrete beams, Struct. J. 90 (1993) 3–11.

[34] R.N. Swamy, R. Jones, A.T.P. Chiam, Influence of steel fibers on the shear resistance of lightweight concrete I-beams, Struct. J. 90 (1993) 103–114.

[35] M. Imam, L. Vandewalle, F. Mortelmans, Shear–moment analysis of reinforced high strength concrete beams containing steel fibres, Can. J. Civ. Eng. 22 (1995) 462–470.

[36] D. Dupont, L. Vandewalle, Shear capacity of concrete beams containing longitudinal reinforcement and steel fibers, Spec. Publ. 216 (2003) 79–94.

[37] C. Cucchiara, L. La Mendola, M. Papia, Effectiveness of stirrups and steel fibres as shear reinforcement, Cem. Concr. Compos. 26 (2004) 777–786.

[38] M.A. Mansur, K.C.G. Ong, P. Paramasivam, Shear strength of fibrous concrete beams without stirrups, J. Struct. Eng. 112 (1986) 2066–2079.

[39] V.C. Li, R. Ward, A.M. Hamza, Steel and synthetic fibers as shear reinforcement, ACI Mater. J. 89 (1992) 499–508.

[40] M. Ahmadi, H. Naderpour, A. Kheyroddin, ANN model for predicting the compressive strength of circular steel-confined concrete, Int. J. Civ. Eng. 15 (2017) 213–221.

[41] H. Naderpour, O. Poursaeidi, M. Ahmadi, Shear resistance prediction of concrete beams reinforced by FRP bars using artificial neural networks, Measurement 126 (2018) 299–308.

[42] N. Karunanithi, W.J. Grenney, D. Whitley, K. Bovee, Neural networks for river flow prediction, J. Comput. Civ. Eng. 8 (1994) 201–220.

[43] K. Hornik, M. Stinchcombe, H. White, Multilayer feedforward networks are universal approximators, Neural Networks. 2 (1989) 359–366.

[44] C. Ferreira, Gene expression programming in problem solving, in: Soft Comput. Ind., Springer, 2002, pp. 635–653.

[45] A. Golbraikh, A. Tropsha, Beware of q2!, J. Mol. Graph. Model. 20 (2002) 269–276.

[46] P.P. Roy, K. Roy, On some aspects of variable selection for partial least squares regression models, Mol. Inform. 27 (2008) 302–313.

[47] M. Ahmadi, H. Naderpour, A. Kheyroddin, A proposed model for axial strength estimation of non-compact and slender square CFT columns, Iran. J. Sci. Technol. Trans. Civ. Eng. 43 (2019) 131–147.

[48] G.N. Smith, Probability and statistics in civil engineering, Collins London (1986).

[49] ACI Committee 544, Design Considerations for Steel Fiber Reinforced concrete, American Concrete Institute (2009).